DATA-DRIVEN NON-LOCAL WAVELET FRAME CONSTRUCTION AND IMAGE RESTORATION

YUHUI QUAN*, HUI JI†, AND ZUOWEI SHEN†

Abstract. By assuming that the interest image can be sparsely approximated in some system, the sparsity-based regularization has been one promising approach emerging in recent years to solving many image restoration problems. One popular system used for sparsely approximating images is the wavelet tight frame which is very efficient for exploiting the sparse nature of local variations of image intensity. However, another powerful image prior often seen in natural images is missing when using existing wavelet frame systems, i.e., the self-recursions of image structures over the whole image. Such a global self-recursive prior of image structures has led to many powerful non-local image restoration schemes with impressive performance. This paper aims at developing a scheme for constructing a non-local wavelet frame or wavelet tight frame that is adaptive to the given image. The constructed non-local wavelet frame, concatenated by one non-local frame and one wavelet tight frame, allows the resulting regularization simultaneously exploits both the sparse prior of local variations of image intensity and the global self-recursive prior of image structures over the image. Based on the proposed construction scheme, a powerful regularization method is developed for solving general image restoration problems. The experiments showed that the results from the proposed regularization method are compared favorably against that from several popular image restoration methods.

Key words. image restoration, wavelets, frame, sparse approximation

AMS subject classifications. 68U10, 65J22,65T60

1. Introduction. Most image restoration tasks are about recovering a high-quality image from its partial and noisy measurement. The measurement is often modeled by a linear operator $A \in \mathbb{R}^{M\times N}$ applied to the input image:

$$g = Af + n, \tag{1.1}$$

where $f \in \mathbb{R}^N$ denote the interest image for recovery, $g \in \mathbb{R}^M$ denote the available measurement of f and $n \in \mathbb{R}^M$ denote the measurement noise. For image noise removal, the matrix A is an identical matrix. For image de-blurring, the matrix A represents a convolution process by a low-pass filter that blurs images. These image recovery problems are usually ill-posed inverse linear problems in which straightforward solutions in term of matrix inversion lead to useless solutions dominated by noise. To solve these ill-posed image restoration problems, certain prior information of the interest image is needed to regularize the recovery process. The sparsity-based prior has been playing a very important role in the recent development of effective image restoration algorithms. The sparsity-based image prior assumes that the interest image is compressible in some transform domain, that is, most of the important information of the image can be kept by using few transform coefficients. Thus, the image recovery process can be regularized by minimizing the functional that prompts the sparsity of the solution in the transform domain. One such convex sparsity promoting functional is the ℓ_1 norm of transform coefficients of the solution. Clearly, the effectiveness of these sparsity-based regularization methods is highly dependent on how efficiently the chosen transform can sparsify the interest image.

*School of Computer Science & Engineering, South China Univ. of Tech., Guangzhou 510006, China

†Department of Mathematics, National University of Singapore, 10, Lower Kent Ridge Road, Singapore 119076, Singapore

In the last few decades, the orthonormal *wavelet bases* [1, 2] have seen their great successes in many image processing tasks, e.g., image compression. However, redundant over-complete systems are often preferred over orthonormal bases in image restoration, as it is empirically observed that the results from over-complete systems tend to be more visually appealing with less artifacts. In recent years, as a generalization of orthonormal wavelet bases, *wavelet tight frames* [3, 4, 5] have been used to sparsely approximate images in many image restoration methods. Many types of wavelet tight frames have been proposed and are applied in various image restoration tasks. For example, shift-invariant wavelet system for image de-noising [6], curvelet [7] and its applications in image de-noising and de-blurring [8, 9], bandlet [10] for image approximation and compression [11], framelet [3, 4] and its applications in many image restoration tasks including in-painting, deblurring and etc (see e.g. [12, 5, 13, 14]). It is noted that the widely used total variation [15] based variational methods are deeply connected with the ℓ_1 norm based regularizations under certain spline framelets. By choosing parameters properly, the analysis approach using spline frames [5] indeed can be viewed as a sophisticated discretization of variational methods involving the total variation penalties (see [16] for more details). The construction of these tight frames relies on certain functional assumptions of images which sometimes are invalid for the particular types of images, an alternative approach is then to adaptively choose the redundant system optimized for the input image. Several adaptive schemes have been developed in recent years. For example, the K-SVD method [17] learns an over-complete system from the input image, and the data-driven tight frame construction method [18] constructs a shift-invariant tight frame optimized for the input image.

The elements of the wavelet frames discussed above are all locally supported in spatial domain. Then, for each image pixel, the associated wavelet frame coefficients measure local image gradients of different degrees in its local neighborhood. In other words, the sparsity prior in the existing wavelet frame systems only refers to the sparse nature of local variations of image intensity. Thus, we may call the existing wavelet frame based regularization and total variation (TV) based regularization a *local* approach. The local approach works well on cartoon-type regions of the image, but leaves plenty of room for improvement on textural regions. An alternative approach is the non-local approach which relates many image pixels that may be far away in spatial domain. The non-local approach is built on one observation often seen in natural images: image structures of small image regions tend to repeat themselves all over the image. Such a prior is non-local in the sense that image pixels from far way may be related to each other. There are two types of non-local schemes proposed to use such a non-local prior. One is the so-called *non-local mean* first introduced in [19] for image de-noising and extended to solve other inverse problems in image processing (see e.g. [20, 21, 22, 23]). The non-local mean approach introduces a non-local operator, e.g. a weighted averaging filter, in the variational model to explore the spatial redundancy. Another is the patch-based approach which groups the similar patches together followed by a collaboratively filtering (see e.g. [24, 25, 26, 27]). One such representative approach is the BM3D method for image de-noising [24] and image deconvolution [25].

The local approaches and the non-local approaches discussed above both have their own advantages and disadvantages. The performance of the local approaches is usually stable and consistent over a wide range of images. Particularly, most local approaches work very well on images dominated by cartoon-type image structures. Also, they can be formulated in a variational framework for solving general linear in-

verse problems with very efficient numerical solvers. However, these local approaches do not work very effectively for images with many textural regions, as these image regions cannot be efficiently approximated in wavelet frame system in a sparse manner. The non-local mean approach addressed such a weakness by introducing a non-local operator in the variational formulation. However, the resulting minimization problem is more challenging to solve than that arising from the local approaches. Also, it is empirically observed that the improvement by introducing an additional non-local operator in the variational formulation often does not justify the additional computational complexity. The performance of the patch-based non-local methods, e.g. the BM3D method, is very impressive in image de-noising and image deconvolution. However, the BM3D method mainly focuses on the global self-recursive prior of image structures, and the sparse nature of local variations of image intensity is not efficiently utilized. As a result, the BM3D method does not work well on images lacking self-recursive image structures, such as fingerprint images.

This paper aims at developing a scheme of constructing a non-local wavelet frame (or tight frame) for the input image to have the best of both the local and non-local worlds. In contrast with existing wavelet frames, the constructed non-local wavelet frame or wavelet tight tight frame is composed of the concatenation of a non-local frame (or tight frame) and a wavelet tight frame, which can facilitate the effective usage of the self-similarities of textural regions in additional to the local sparsity prior of image gradients. Built upon the proposed construction scheme of non-local wavelet frame, a variational image restoration method is then developed to exploit both the sparsity prior of local intensity variations and the global self-similarities of image structures. Different from the non-local mean method, the proposed regularization method does not require the development of sophisticated numerical solvers. Many existing fast numerical algorithms for solving ℓ_1 norm related minimization problems, e.g. the split Bregman iteration [28, 29], can be applied in a straightforward manner. Different from many existing patch-based methods, the proposed variational formulation works for general image restoration problems and is applicable to a wide range of images, including those lacks self-recursive image structures. The experimental evaluation also showed that the proposed regularization method is compared favorably against some popular local and non-local image restoration methods in terms of both PSNR value and visual quality. The rest of the paper is organized as follows. In Section 2, we give a brief review on frame, wavelet frame, tight frame, local and non-local image restoration schemes . The main results are presented in Section 3. Section 4 is devoted to the experimental evaluation of the proposed method.

2. Preliminaries and previous work.

2.1. Wavelet frame, tight frame and image restoration. We first present here some basics of frame and tight frame in a Hilbert space H. Interested readers are referred to [4, 5, 30] for more details. Let $\langle\cdot,\cdot\rangle$ and $\|\cdot\|$ denote the usual inner product and norm of a Hilbert space $\mathcal{H}$. A sequence $\{\phi_n\}_{n\in\mathbb{N}} \subset \mathcal{H}$ is a frame for $\mathcal{H}$ if there exist two positive constants a and b such that

$$a\|f\|_2^2 = \sum_{n\in\mathbb{N}} |\langle\phi_n, f\rangle|^2 \leq b\|f\|_2^2, \quad \forall\, f \in \mathcal{H}.$$

A frame $\{\phi_n\}_{n\in\mathbb{N}}$ is called a tight frame for H when $a = b = 1$. There are two operators associated with a given frame $\{\phi_n\}_{n\in\mathbb{N}}$: the analysis operator W defined by

$$W : f \in \mathcal{H} \longrightarrow \{\langle f, \phi_n\rangle\} \in \ell^2(\mathbb{N})$$

and its adjoint operator W^*, also called the synthesis operator, defined by

$$W^* : \{a_n\} \in \ell^2(\mathbb{N}) \longrightarrow \sum_n a_n \phi_n \in \mathcal{H}.$$

The concatenation of these two operators forms a so-called frame operator $S = W^*W$ given by

$$S : f \in \mathcal{H} \longrightarrow \sum_{n\in\mathbb{N}} \langle f, \phi_n\rangle \phi_n.$$

Thus, a sequence $\{\phi_n\} \subset \mathcal{H}$ forms a frame if and only if $aI \leq S \leq bI$ and it forms a tight frame if and only if $S = I$, where $I : \mathcal{H} \longrightarrow \mathcal{H}$ is the identical operator. Frame can be viewed as a generalization of Riesz Basis and tight frame is a redundant system that generalizes orthonormal basis. Indeed, a given tight frame $\{\phi_n\}_{n\in\mathbb{N}}$ has the same perfect reconstruction property as orthonormal basis:

$$f = \sum_{n\in\mathbb{N}} \langle f, \phi_n\rangle \phi_n, \quad \forall\, f \in \mathcal{H}. \tag{2.1}$$

and it becomes an orthonormal basis if $\|\phi_n\| = 1$ for all ϕ_n.

One widely used tight frame in signal/image processing is wavelet tight frame. The wavelet tight frame for $L_2(\mathbb{R})$ is the system formed by the shifts and dilations of a finite set of generators $\Psi = \{\psi_1, \ldots, \psi_m\} \subset L_2(\mathbb{R})$:

$$X(\Psi) = \{2^{j/2}\psi_\ell(2^j \cdot -k), \quad 1 \leq \ell \leq m, j \in \mathbb{Z}, k \in \mathbb{Z}\}.$$

Framelets are the wavelet tight frames constructed via multi-resolution analysis, which starts with a scaling function ϕ with $\widehat{\phi}(0) = 1$ that satisfies the following refinable equation satisfying

$$\widehat{\phi}(2\cdot) = \widehat{a_0}\widehat{\phi},$$

where $\widehat{\phi}$ is the Fourier transform of ϕ, and $\widehat{a_0}$ is a 2π-periodic trigonometric polynomial

$$\widehat{a_0}(\omega) := \sum_{k\in\mathbb{Z}} a_0(k) e^{-ik\omega}$$

with $\widehat{a_0}(0) = 1$. Then the generators $\{\psi_1, \ldots, \psi_m\}$ is defined by

$$\widehat{\psi_\ell} = \widehat{a_\ell}\widehat{\phi}, \quad 1 \leq \ell \leq m.$$

The so-called Unitary Extension Principle ([3]) states that $X(\Psi)$ forms a tight frame provided that $\phi \in L^2(\mathbb{R})$ and

$$\sum_{\ell=0}^{m} \widehat{a}_\ell(\omega)\overline{\widehat{a_\ell}(\omega + \pi\gamma)} = \delta_\gamma, \quad \gamma = 0, 1. \tag{2.2}$$

One widely used wavelet tight frame in many applications is the linear B-spline framelet (see e.g. [31, 12, 32]) with two generators and the associated masks $\{a_0, a_1, a_2\}$ are

$$a_1 = \frac{1}{4}[1, 2, 1]; a_2 = \frac{\sqrt{2}}{4}[1, 0, -1]; a_3 = \frac{1}{4}[-1, 2, -1]. \tag{2.3}$$

The framelet system for $L_2(\mathbb{R}^2)$ can be obtained by taking the tensor product of univariate framelets.

In the discrete setting, for a given frame $\{\phi_n\}_{n=1}^M \subset \mathbb{R}^N$, the matrix representation of the associated analysis operator is $W = (\phi_1, \phi_2, \ldots, \phi_M)^\top$ and the synthesis operator is its transpose $W^\top$. Clearly, $\{\phi_n\}_{n=1}^M$ forms a frame for $\mathbb{R}^N$ if and only if $W^\top W$ is non-singular and it forms a tight frame if and only if $W^\top W = I_N$, where I_N is the N-by-N identical matrix. The wavelet tight frame for $\mathbb{R}^N$ can be constructed from the masks associated with the framelets for the space of continuum. For simplicity, only single-level un-decimal wavelet tight frame system for $\mathbb{R}^N$ is introduced. Let $\{a_0, a_1, \ldots, a_m\}$ denote the masks associated with the framelet system Ψ with finite support. Let $f \in \mathbb{R}^N$ denote the vector form of the image by concatenating all columns of $\mathbf{f}$ into a single column vector. For a given filter a of finite length, Let the N-by-N matrix, denoted by $\mathcal{S}_a$, be the Toeplitz matrix that represents the convolution operator by the mask a under Neumann boundary condition. Then, the columns of the following N-by-$(m+1)N$ matrix:

$$[\mathcal{S}_{a_0}, \mathcal{S}_{a_1}, \ldots, \mathcal{S}_{a_m}] \tag{2.4}$$

forms a tight frame for $\mathbb{R}^N$. Let W denote the transpose of (2.4), then W is the analysis operator and its transpose $W^\top$ is the synthesis operator of the tight frame system (2.4). The perfect reconstruction property in matrix representation can be expressed as $W^\top W = I_N$.

Image restoration is about solving the ill-posed linear system (1.1) with some additional regularization on the solution. There are several approaches for wavelet frame based regularization, namely the synthesis based approach, the analysis based approach and the balanced approach; see [33, 5] for more details. Here we focus on the analysis based approach which solves (1.1) via solving the following minimization model:

$$\operatorname*{argmin}_f \frac{1}{2}||g - Af||_2^2 + ||\operatorname{diag}(\lambda) W f||_1, \tag{2.5}$$

where W is the analysis operator of some discrete wavelet frame system. and λ is the weighting vector. In order to successfully recover the interest image from (1.1) via solving (2.5), the interest image should have a good sparse approximation under the discrete wavelet frame system. Many efficient algorithms have been developed in recent years to solve (2.5), e.g. the split Bregman iteration method [28, 29].

2.2. Related non-local image restoration schemes. There have been an abundant research literature on patch-based methods for various image restoration tasks. In this section, we will only discuss the most related work. The basic idea of most non-local methods in image processing is to recover the degraded pixel using other similar pixels. The non-local means (NLM) is first introduced by Buades *et al.* [19] for image de-noising. In the continuous setting, the non-local means method introduces a neighborhood de-noising filter applied on the image:

$$NL_f(x) := \Big(\int_\Omega \omega_f(x,y)dy\Big)^{-1} \int_\Omega \omega_f(x,y) f(y) dy. \tag{2.6}$$

where f is the reference image and ω_f is the weight function given by

$$\omega_f(x,y) = \exp\Big(-\frac{G_\sigma * |f(x+\cdot) - f(y+\cdot)|^2(0)}{h^2}\Big),$$

where G_σ is the Gaussian kernel with s.t.d. σ and h are the filtering parameters associated with noise level. It is seen that the weights are significant only when the patch around y is similar to the corresponding patch around x. As a result, the self-similarity of image patches are used for noise deduction. The non-local means method is extended in [22] to address more general image restoration problems such as image deconvolution:

$$\text{argmin}_f \frac{\lambda}{2}\int_\Omega (k*f-g)^2 + \int_\Omega (\int_\Omega \sqrt{(f(x)-f(y))^2\omega_f(x,y)dy})dx. \tag{2.7}$$

The regularization term in the above minimization clearly is a generalization of the TV based regularization by applying a neighborhood de-noising filter on TV measures.

A representative patch-based non-local scheme is the BM3D method [24, 25]. The basic steps of the BM3D de-noising method [24] are as follows. First similar image blocks are stacked in a 3D array based on the sum-of-squares distance function between different image patches. Then a collaborative filtering is carried out on each 3D image stack to suppress noise. For example, a shrinkage in 3D transform domain such as wavelet shrinkage or Wiener filtering. The de-noised image is then synthesized from the de-noised patches after inverting 3D transform. The result is then further refined by iteratively doing the grouping and collaboratively filtering. For image deconvolution, the BM3D deblurring method [25] takes a two-step approach. (i) The first step is to estimate an initial de-blurred result using the regularized inverse in discrete Fourier domain, followed by a de-noising process using the BM3D method with collaborative hard thresholding. Then this initial de-blurred result is used to synthesize a blurred image with better signal-to-noise ratio. (ii) Taking this re-estimated blurred image as the input, the second step is to re-estimate the result using the regularized Wiener filter, followed by a de-noising process using the BM3D method with collaborative Wiener filtering. The BM3D method is a very effective image restoration scheme with state-of-the-art performance.

3. Main results. Image restoration is about estimating the true image f from the linear system (1.1). In most image restoration problems, the matrix A in (1.1) is an ill-conditioned or non-invertible matrix. By assuming that the frame coefficient vector of the true solution f tends to be sparse, one popular sparsity-based approach is the so-called analysis based approach (e.g. [33, 5, 28, 29]), which estimates f by solving the following ℓ_1 norm related minimization model:

$$\min_f \Phi(g-Af) + ||\operatorname{diag}(\lambda)Df||_1, \tag{3.1}$$

where λ is some regularization parameter vector and D is the analysis operator of some frame system. There are two terms in the above minimization. The first term is the fidelity term and the functional Φ is set as $\frac{1}{2}\|\cdot\|_2^2$ when assuming only i.i.d. Gaussian white noise. The second term is the weighted ℓ_1 norm of coefficients which approximately measures the sparsity of the canonical frame coefficient vector Df. The performance of the model (3.1) largely depends on how well the analysis operator D can sparsify the true image f.

In this section, we first presented a scheme for constructing the analysis operator W of non-local discrete wavelet frames and tight frames for $\mathbb{R}^N$, under which the regularization method such as (3.1) can exploit both local sparsity prior of images in wavelet tight frame domain and the global self-recursion of image structures. Then, built on the introduced non-local wavelet frame system, a numerical method is developed for solving general image restoration problems.

3.1. Construction scheme of adaptive non-local wavelet tight frame and frame. Many types of wavelet tight frames have been used for image restoration, including translation-invariant wavelets system [6] and spline framelets [12, 13, 14]. In the discrete case, these wavelet tight frame systems are generated by the shifts of several filters of small localized support, which are very suitable for sparsely approximating cartoon-type image regions composed of sparsely distributed edges. However, their effectiveness significantly decreases when approximating textural regions composed of dense small edge segments. For these textural regions, a more efficient approach is to represent the dense image structures of these regions by themselves since these image structures are likely to repeat themselves over the image. Notice that if we represent these image structures under a wavelet tight frame, the associated wavelet tight frame coefficients will also have the same self-recursive property. Thus, by assuming the likely self-recursions of wavelet tight frame coefficients, we propose a frame system (or tight frame system) whose analysis operator is of the form

$$D(f) = \frac{1}{\sqrt{2}} \begin{pmatrix} I \\ J(f) \end{pmatrix} W = \frac{1}{\sqrt{2}} \begin{pmatrix} W \\ J(f)W \end{pmatrix} \tag{3.2}$$

where $W \in \mathbb{R}^{M\times N}$ is the analysis operator associated with some existing wavelet frame system (e.g. shift-invariant cubic spline framelet [3]), $I \in \mathbb{R}^{M\times M}$ is the identical matrix, and $J(f) \in \mathbb{R}^{M\times M}$ is the operator that encodes the global self-recursive property of wavelet tight frame coefficients Wf.

The proposed frame system of the form (3.2) is formed by concatenating two systems: one is some existing discrete wavelet tight frame system denoted by W, and the other is a modified version of W by applying an operator $J(f)$. Since the discrete wavelet tight frame systems are generated by the shifts of the finitely-supported wavelet filters, the non-zero elements of each row of the matrix W are then agglomerated into some local interval. Thus, we may call the tight frame formed by the rows of W a *local* wavelet tight frame. The operator $J(f)$ is used for relating the wavelet frame coefficients corresponding to the same image structure, which often are not agglomerating in neighboring regions but rather are spreading out over the whole image. Thus the operator $J(f)$ can be viewed as a non-local operator to relate wavelet frame coefficients that may be spatially far away from each other, and the rows of $J(f)W$ can be viewed as a non-local version of discrete wavelet frame system generated by W. Therefore, we may call the frame (tight frame) of the form (3.2) a *non-local* wavelet frame (tight frame).

PROPOSITION 1. *Let $W \in \mathbb{R}^{M\times N}$ be a tight frame system satisfying $W^\top W = I_N$. For any $f \in \mathbb{R}^N$, define $D(f)$ by* (3.2)*. Then the rows of D form a frame system for $\mathbb{R}^N$, and they form a tight frame system for $\mathbb{R}^N$ provided that $J(f)^\top J(f) = I_M$.*

Proof. Notice that

$$\begin{aligned} S &= D(f)^\top D(f) \\ &= \frac{1}{2} W^\top (I + J(f)^\top J(f)) W \\ &= \frac{1}{2} W^\top W + \frac{1}{2} W^\top J(f)^\top J(f) W \\ &= \frac{1}{2} I + \frac{1}{2} W^\top J(f)^\top J(f) W. \end{aligned}$$

Since the term $\frac{1}{2} W^\top J(f)^\top J(f) W$ is positive semi-definite, the matrix S is a positive definite matrix. Thus, the rows of $D(f)$ forms a frame for $\mathbb{R}^N$. Moreover, if

$J(f)^\top J(f) = I_M$, then we have

$$S = \frac{1}{2} I_N + \frac{1}{2} W^\top J(f)^\top J(f) W = \frac{1}{2} I_N + \frac{1}{2} W^\top W = I_N.$$

Thus, the rows of $D(f)$ forms a tight frame for $\mathbb{R}^N$. ∎

Proposition 1 states that the system formed by (3.2) is always a frame and is a tight frame if $J(f)$ is the analysis operator of some tight frame system. In the next, we give a detailed description on how to construct a non-local operator $J(f)$ whose rows form a tight frame for $\mathbb{R}^M$. First, the wavelet frame coefficient vector Wf is divided into different sub-sets such that each sub-set only contains the wavelet frame coefficients from the same wavelet channel and corresponding to the same image structure. In other words, two tight frame coefficients belong to the same set if

(i) they both belong to the same wavelet channel, i.e., they are the outputs of applying the same wavelet filter a_ℓ on the image;

(ii) the image regions related to the calculation of these two coefficients are the same.

Let $\{\mathcal{G}_\ell\}_{\ell=1}^L$ denote the index sets of these coefficient sets and let $J_0 \in \mathbb{R}^{M\times M}$ defined by

$$J_0(j,k) = \frac{1}{K_\ell} \begin{cases} -(K_\ell - 2), & j = k; \\ 2, & j \neq k \text{ and } j,k \in \mathcal{G}_\ell; \\ 0, & \text{otherwise}, \end{cases} \tag{3.3}$$

where K_ℓ denotes the cardinality of the set $\mathcal{G}_\ell$. Define the operator $D(f)$ by

$$D(f) = \frac{1}{\sqrt{2}} \begin{pmatrix} I \\ J(f) \end{pmatrix} W = \frac{1}{\sqrt{2}} \begin{pmatrix} W \\ \operatorname{diag}(\mu) J_0 W \end{pmatrix} \tag{3.4}$$

where $\mu \in \mathbb{R}^M$ is defined as $\mu(j) = 1/K_\ell$ for $j \in \mathcal{G}_\ell$. Then such an operator $D(f)$ is indeed an analysis operator of a tight frame for $\mathbb{R}^N$.

Proposition 2. *Let $W \in \mathbb{R}^{M\times N}$ be a tight frame system satisfying $W^\top W = I_N$. For any $f \in \mathbb{R}^N$, the rows of $D(f)$ defined by (3.4) forms a tight frame for $\mathbb{R}^N$.*

Proof. Let P be the permutation matrix such that it permutes the index vector $(1,\dots,M)^\top$ into the vector concatenated by all index sets $\{\mathcal{G}_\ell\}_{\ell=1}^L$:

$$(\mathcal{G}_1^\top, \dots, \mathcal{G}_L^\top)^\top.$$

Let $J(f) = \operatorname{diag}(\mu) J_0$, then we have

$$P^\top J(f) = \operatorname{diag}(J_1, J_2, \dots, J_L),$$

where $J_\ell \in \mathbb{R}^{K_\ell \times K_\ell}$ given by

$$J_\ell = \frac{1}{K_\ell} \begin{pmatrix} 2-K_\ell & 2 & \cdots & 2 & 2 \\ 2 & 2-K_\ell & \cdots & 2 & 2 \\ 2 & 2 & \ddots & 2 & 2 \\ \vdots & \vdots & \vdots & \vdots & \vdots \\ 2 & 2 & \cdots & 2 & 2-K_\ell \end{pmatrix}.$$

A direct calculation leads to ${J_\ell}^\top J_\ell = I_{K_\ell}$. Thus,

$$\begin{aligned} J(f)^\top J(f) &= \operatorname{diag}(J_1, J_2, \dots, J_L)^\top P^\top P \operatorname{diag}(J_1, J_2, \dots, J_L) \\ &= \operatorname{diag}(J_1^\top J_1, \dots, J_L^\top J_L) \\ &= I_M. \end{aligned}$$

By Proposition 1, the rows of $D(f)$ forms a tight frame for $\mathbb{R}^N$. □

It is seen from the above construction scheme that the non-zero elements of each row of the operator $J(f)$ sparsely spread out over the whole row. As a result, the tight frame formed by $J(f)W$ also becomes non-local, as for each row, its non-zero elements also spread out over the whole row. Indeed, as we show in the following, the outcome $J(f)Wf$ is a non-local version of wavelet tight frame coefficient vector Wf. By the definition of $\mathcal{G}_\ell$, we have that

$$(Wf)(j) = (Wf)(k), \text{for any } j,k \in \mathcal{G}_\ell$$

which is equivalent to

$$(Wf)(j) = \frac{1}{K_\ell}\Big(\big(\sum_{k\neq j, k\in\mathcal{G}_\ell} 2(Wf)(k)\big) - (K_\ell - 2)Wf(j)\Big), \quad \forall\, j \in \mathcal{G}_\ell, \tag{3.5}$$

or in the matrix form:

$$Wf = J(f)Wf.$$

Thus, when we use $D(f)$ defined by (3.4) in the regularization model (3.1), the regularization functional includes two components:

$$\begin{aligned} \|\operatorname{diag}(\lambda)D(f)f\|_1 &= \|\begin{pmatrix} \operatorname{diag}(\lambda_1) \\ \operatorname{diag}(\lambda_2)J(f) \end{pmatrix} Wf\|_1 \\ &= \|\operatorname{diag}(\lambda_1)Wf\|_1 + \|\operatorname{diag}(\lambda_2)J(f)Wf\|_1. \end{aligned} \tag{3.6}$$

The first component is the local version of the weighted ℓ_1 norm of wavelet tight frame coefficients and the second component is the non-local version of the weighted ℓ_1 norm of wavelet tight frame coefficients. Compared to the widely used regularization functional $\|\operatorname{diag}(\lambda)Wf\|_1$, the new functional $\|\operatorname{diag}(\lambda)D(f)f\|_1$ not only enforces the same local sparsity prior of the image f in wavelet tight frame domain, but also enforces an additional non-local constraint on the self-recursions of wavelet frame coefficients.

There are a few issues to be addressed when directly using the tight frame $D(f)$ constructed by (3.4) in image restoration. One is the un-availability of the true image f in image restoration. Often we only have a rough estimate of f in hand which may contain noticeable errors in the early stage. Another one is the imperfection of self-recursions of image structures in practice. The image structures are usually not exactly repeating themselves but rather they are highly similar. Thus, we propose a modified version of $D(f)$ to address both the errors in the estimate of f and the imperfection of self-recursing image structures. The modified frame system, is still of the form (3.4) but with a slightly different non-local operator $J(f)$. The first modification is on the definition of $\{\mathcal{G}_\ell\}_{\ell=1}^L$. Instead of grouping only wavelet coefficients corresponding to the same image structure, we group the wavelet coefficients corresponding to image structures with high similarity. Secondly, we introduce the weights into the definition of J to measure the similarity degree of wavelet frame coefficients. The modified non-local operator, denoted by $\widetilde{J}$, is defined as follows,

$$\widetilde{J}(j,k) = \frac{1}{\omega(j,\mathcal{G}_\ell)+1}\begin{cases} -(\omega(j,\mathcal{G}_\ell)-1), & j = k; \\ 2\omega(j,k), & j \neq k \text{ and } j,k \in \mathcal{G}_\ell; \\ 0, & \text{otherwise.} \end{cases} \tag{3.7}$$

where $0 < \omega(j,k) \leq 1$ is the weight defined by some similarity measurement between two wavelet tight frame coefficients, and $\omega(j,\mathcal{G}_\ell) = \sum_{k\neq j, k\in\mathcal{G}_\ell} \omega(j,k)$. It is seen that the definition of (3.7) is degenerated to (3.3) of the ideal case where all weights are the same. In summary, we propose a modified version of the operator $D(f)$ for better performance when solving practical image restoration problems:

$$D(f) = \frac{1}{\sqrt{2}} \begin{pmatrix} I \\ \widetilde{J}(f) \end{pmatrix} W \tag{3.8}$$

where $\widetilde{J}(f)$ is defined by (3.7) and W is the analysis operator of some wavelet tight frame system. By proposition 1, the new operator $D(f)$ of the form (3.8) is the analysis operator of a frame system for $\mathbb{R}^N$.

3.2. Minimization model and regularization method for image restoration. For image restoration, the non-local adaptive tight frame proposed in the previous section cannot be pre-constructed as the true image f is not available. Thus, we propose the following minimization model for solving the ill-posed linear system (1.1):

$$\operatorname{argmin}_{f\in\mathbb{R}^N} \frac{1}{2}\|Af-g\|_2^2 + \|\operatorname{diag}(\lambda)D(f)\|_1, \tag{3.9}$$

where D is defined by (3.8). We take an iterative scheme to alternatively update the estimation of f and the operator $D(f)$. See Algorithm 1 for the outline of the iterative scheme. There are two non-trivial steps in Algorithm 1, one is using the current estimate $f^{(k)}$ of the true image to construct the index sets $\{\mathcal{G}_\ell^{(k)}\}_{\ell=1}^L$ and another is to re-estimate the true image by solving the minimization model (3.9) with $D(f) := D^{(k)}$. The construction of $\{\mathcal{G}_\ell^{(k)}\}_{\ell=1}^L$ in first step requires solving a discrete optimization problem. Regarding the minimization problem (3.9), many efficient numerical solvers have been developed for solving such type of minimization problems in recent years, e.g, the split Bregman iteration [28, 29].

Algorithm 1 Alternative iteration scheme for solving (3.9)

Input: the degraded image g
Output: the recovered image f
Main procedure:

1. $f^{(0)} := g$.
2. for $k = 0, 1, \ldots, K-1$
   (a) constructing the index sets of groups $\{\mathcal{G}_\ell^{(k)}\}_{\ell=1}^L$ using $f^{(k)}$;
   (b) synthesizing $D^{(k)}$ defined by (3.8) and (3.7) using $\{\mathcal{G}_\ell^{(k)}\}_{\ell=1}^L$;
   (c) $f^{(k+1)} := \operatorname{argmin}_{f\in\mathbb{R}^N} \frac{1}{2}\|Af-g\|_2^2 + \|\operatorname{diag}(\lambda)D^{(k)}f\|_1$.
3. $f := f^{(K)}$.

In the computation, a rigorous construction of $\{\mathcal{G}_\ell^{(k)}\}_{\ell=1}^L$ is a very time consuming process. Certain simplifications are needed such that the construction provides a reasonable good grouping within acceptable running time. In our implementation, for computational efficiency, all index sets $\mathcal{G}_\ell$s have the same size S and for each framelet coefficient, only the first $S-1$ framelet coefficients in its neighborhood with the highest similarity are grouped together. The similarity measure between two

framelet coefficients is defined as the square difference summation of two image regions associated with these two coefficients:

$$\omega(\Omega_1,\Omega_2)=\exp(-\sum_{j\in\Omega_1,i\in\Omega_2}(f^{(k)}(j)-f^{(k)}(i))^2/h_0). \tag{3.10}$$

where Ω_1 and Ω_2 are two image regions contains all image pixels related involved in the calculation of the framelet coefficient, h is some constant (set to 3/10 in our implementation). Take for example the single-level cubic framelet system. For each cubic spline framelet coefficient, only a 5×5 image region is involved in the calculation and we define this image region the region Ω_0 or Ω_1 used in (3.10).

The error in the initial estimates $f^{(k)}$ will also have a negative impact on the performance of the deconvolution process by (3.9). The negative impact mainly comes from the relatively low quality of the non-local operator $\widetilde{J}(f)$ in the frame system $D^{(k)}$. Thus, we propose to update the regularization parameter vector $\lambda^{(k)}$ during each iteration according to the accuracy of the operator $D^{(k)}$. In our implementation, we propose the following empirical formulation of setting the regularization parameter vector $\lambda^{(k)}\in\mathbb{R}^{2M}$:

$$\lambda^{(k)}=\begin{pmatrix}\lambda_1^{(k)}\\ \lambda_2^{(k)}\end{pmatrix} \tag{3.11}$$

where

$$\begin{cases}\lambda_1^{(k)}(j)=\lambda_0\frac{\sigma_n}{\sqrt{\eta+\max(0,\frac{1}{S}\sum\limits_{j,i\in\mathcal{G}_l}|Wf^{(k)}(i)|^2-\sigma_n^2)}}\\ \lambda_2^{(k)}(j)=c_0^{-1}\lambda_0\frac{\sigma_n}{\sqrt{\eta+\max(0,\mathrm{var}(\{Wf^{(k)}(i):j,i\in\mathcal{G}_l\})-\sigma_n^2)}}\end{cases}\qquad 1\le j\le M. \tag{3.12}$$

In (3.12), the variable σ_n denotes the standard deviation of image noise which could be estimated in many image restoration tasks by some statistical approach (see e.g. [34]). The operator $\mathrm{var}(\cdot)$ denotes the variance estimator. There are three constants in (3.12): λ_0, c_0, η. The constant λ_0 is the regularization value; the constant c_0 determines the percentage of local and non-local constraints in the overall regularization; the constant η is just for numerical stability. Once the regularization parameter vector $\lambda^{(k)}$ is set, the minimization (3.9) can be solved by split Bregman iteration. A detailed description for the proposed regularization method is summarized in Algorithm 2.

4. Experiments and discussions. Algorithm 2 can be used to solve general image restoration problems. In this section, we will mainly focus on the evaluation of Algorithm 2 in the application of image deconvolution. The applications of Algorithm 2 in image de-noising and image in-painting will be demonstrated only with a few examples.

Let $\mathbf{f}$, $\mathbf{g}$ denote the true image and the observed image, and let $f,g\in\mathbb{R}^N$ denote their vectorized versions. where $n\in\mathbb{R}^N$ denotes image noise. For image deconvolution, the matrix A in the linear system (1.1) becomes the convolution operator, i.e., the blurring process can be modeled as a convolution process such that

$$\mathbf{g}=\mathbf{p}*\mathbf{f}+\mathbf{n}, \tag{4.1}$$

where $\mathbf{p}$ denotes the blur kernel and '$*$' denotes the 2D discrete convolution operator. The system (4.1) can be re-written in the matrix form:

$$g=Af+n, \tag{4.2}$$

Algorithm 2 Regularization method using non-local tight frames

Input: the observed image g

Output: the recovered image f

Main procedure:

1. $f^{(0)} := g$.
2. For $k = 1, ..., K$,
   (a) constructing the index sets of groups $\{\mathcal{G}_\ell^{(k)}\}_{\ell=1}^L$ using $f^{(k)}$.
   (b) synthesizing $D^{(k)}$ using (3.8).
   (c) $d^{(0)} = b^{(0)} := \mathbf{0}$ and $D := \widetilde{D}^{(K)}$.
   (d) For $p = 1, ..., P$,
      i. synthesizing $\lambda^{(k)}$ using (3.11) and (3.12).
      ii. defining

$$\begin{cases} u^{(p)} := (A^TA + \mu D^TD)^{-1}(A^Tg + \mu D^T(d^{(p-1)} - b^{(p-1)})); \\ d^{(p)} := T_\lambda(Du^{(p)} + b^{(p-1)}); \\ b^{(p)} := b^{(p-1)} + \delta(Du^{(p)} - d^{(p)}), \end{cases},$$

   where μ and δ are two parameters used in split Bregman iteration, and T_λ is the soft-thresholding operator defined by

$$T_\lambda(u) = \text{sign}(u)\max(|u| - \lambda, 0).$$

   (e) $f^{(k)} := u^{(P)}$.
3. $f := f^{(K)}$.

peppers256 goldhill256 boat256 camera256

house256 fingerprint512 Lena512 Barbara512

FIG. 4.1. *Eight tested images*

where A is a block-wise Toeplitz matrix under Neumann boundary extension or a block-wise circulant matrix under periodic boundary extension.

4.1. Experiments and demonstrations. For the experiments on image deconvolution, we run Algorithm 2 on eight images as shown in Figure 4.1. The experimental setup is as follows. Each tested image is first convoluted by a blur kernel, followed by the addition of Gaussian white noise with different standard deviations.

Four different types of blur kernels are tested in the experiments, including (a) a disk kernel of radius 3 pixels; b) a linear motion kernel of length 15 pixels and orientation 30°; (c) a Gaussian kernel of size 25×25 pixels and standard deviation $8/5$; and (d) a box kernel of size 9×9 pixels. The mathematical expression of a 2D Gaussian blur kernel is $p(r) = (2\pi\sigma^2)^{-1} \exp(-\|r\|_2^2/(2\sigma^2))$. The other three blur kernels can be expressed as

$$\mathbf{p}(r) = \frac{1}{\#\Omega} \begin{cases} 1, & r \in \Omega, \\ 0, & \text{otherwise}, \end{cases}$$

where ω is the support of the kernel, which is a disk, a box and a line segment respectively; and $\#\Omega$ denotes the cardinality of Ω. We use the peak signal to noise ratio (PSNR) as the quantitative measure of image quality which is defined by

$$\text{PSNR}(f, \hat{f}) = -20\log_{10} \frac{||f - \hat{f}||_2^2}{255N},$$

where f is the true image, $\hat{f}$ is the restored image and N is the total number of image pixels.

The experimental results from Algorithm 2 are compared to that from three related existing image restoration approaches. The first is the framelet based image restoration approach [29] which also uses the same minimization model (3.9) to recover the true image. The main difference between the framelet based method and Algorithm 2 lies in the choice of the wavelet frame system D in the model (3.9). The former uses the linear spline wavelet frame system and the later uses the non-local wavelet frame system of the form (3.8). The second method for comparison is the non-local TV based approach [22] which introduces a non-local mean operator into the TV-based image regularization. The third one is the patch-based BM3DDEB approach introduced in [25], the generalization of the BM3D method to image deconvolution. The BM3DDEB method is built on the concept of collaborative filtering on the 3D array of matched image patches. The results from three methods for comparison are all generated by using the codes from the original authors which are available online.

The same parameters of Algorithm 2 are used for all eight input images during the experiments. As we observed in the experiments, only one more round of the refinement for patch matching is sufficient to obtain satisfactory results. Thus, the iteration number K of outer loops is set to 2. The iteration number P of the inner loops is set to 100. The two parameters μ and δ for the spilt Bregman iteration are set to $1/10$ and 1 respectively. The parameters of the adaptive regularization vector defined in (3.12) are set to $\eta = 3/10$, $\lambda = 0.078$ and $c_0 = 6/5$. The fact that $c_0 > 1$ implies that the ℓ_1 norm of the non-local wavelet frame coefficients take a larger percentage of the regularization in (3.9) than that of local wavelet frame coefficients.

Table 4.1 and 4.2 summarize the PSNR values of the results de-blurred by four methods, with respect to different configurations on blur kernels and noise levels. It is seen that Algorithm 2 outperformed the framelet method and the non-local TV method by a large margin in most test images. Also it outperformed the BM3DDEB method in most test images, but it did not perform as well as the BM3DDEB method on the image "Barbar512". The main reason is that the BM3DDEB method enforces the sparsity constraint in DCT transform, which is very suitable for representing the stripe textures that are prevailing in the image "Barbar512". For the images

Image	Kernel	Local framelet	Nonlocal TV	BM3DDEB	Algorithm 2
peppers256	disk	28.43	28.08	30.35	**31.76**
	motion	28.35	27.25	29.53	**31.50**
	gaussian	26.73	26.75	27.19	**28.35**
	box	28.46	27.60	28.55	**29.80**
goldhill256	disk	27.66	27.63	27.87	**28.07**
	motion	27.66	26.97	27.41	**28.33**
	gaussian	27.10	27.28	27.38	**27.66**
	box	26.87	26.57	26.89	**27.32**
boat256	disk	26.88	27.06	27.13	**27.74**
	motion	26.75	26.59	26.92	**27.88**
	gaussian	26.31	26.72	26.57	**26.96**
	box	25.64	25.72	25.93	**26.34**
camera256	disk	27.45	28.06	28.54	**29.49**
	motion	27.63	27.57	28.29	**29.61**
	gaussian	26.39	27.00	27.08	**27.60**
	box	25.77	26.12	26.61	**27.15**
house256	disk	32.98	32.51	33.54	**34.71**
	motion	32.10	31.13	32.72	**34.28**
	gaussian	31.80	32.41	32.41	**33.53**
	box	31.79	30.71	32.32	**33.45**
fingerprint512	disk	29.23	28.25	28.76	**29.45**
	motion	27.84	25.45	26.49	**28.20**
	gaussian	29.79	29.75	29.53	**30.06**
	box	26.28	25.00	25.03	**26.30**
Barbara512	disk	25.47	25.76	**27.60**	26.33
	motion	25.49	25.48	**27.99**	26.86
	gaussian	24.58	24.70	**25.05**	24.71
	box	24.30	24.31	**25.01**	24.61
Lena512	disk	32.91	31.82	32.91	**33.90**
	motion	32.03	30.46	32.03	**33.27**
	gaussian	33.05	32.90	33.05	**33.94**
	box	30.68	30.01	31.06	**31.54**

TABLE 4.1

Comparison of the PSNR values (dB) of the results by four methods, with respect to the noise level $\sigma = 2$.

dominated by other types of texture or dominated by cartoon-type regions, Algorithm 2 performed noticeably better, for example the image "fingerprint512" and the image "peppers256". The reason is that the self-recursive property of image structures is very weak on these two images which results in poorly matched patches in the BM3DDEB method. Contrary to the BM3DDEB method, the non-local wavelet frame system used in Algorithm 2 allows the simultaneous usage of both the local prior in wavelet frame domain and the non-local prior of wavelet frame coefficients. Together with the regularization parameters adaptive to the accuracy of each prior, Algorithm 2 performs consistently on a wide range of images, including both image of rich textures and images of less textures. The advantage of Algorithm 2 over other methods in terms of the PSNR value is also consistent with the improvement of the visual quality. See Figures 4.2, Figure 4.3 and Figure 4.4 for the visual comparison of the results on a few tested images.

Algorithm 2 can also be applied to solve many other image restoration problems

Image	Kernel	Local framelet	Nonlocal TV	BM3DDEB	Algorithm 2
peppers256	disk	26.14	25.22	28.08	**29.25**
	motion	25.41	24.20	26.60	**28.26**
	gaussian	25.97	25.65	26.29	**27.66**
	box	25.84	25.45	26.67	**27.78**
goldhill256	disk	26.31	25.43	26.65	**26.69**
	motion	25.78	24.44	25.95	**26.19**
	gaussian	26.33	26.29	26.59	**26.83**
	box	25.40	24.87	25.69	**25.78**
boat256	disk	25.23	24.91	25.71	**25.75**
	motion	24.61	23.88	25.06	**25.24**
	gaussian	25.40	25.58	25.64	**25.81**
	box	24.19	24.20	24.56	**24.62**
camera256	disk	25.43	25.43	26.50	**26.82**
	motion	24.97	24.33	25.82	**26.48**
	gaussian	25.44	25.91	26.02	**26.26**
	box	24.16	24.46	24.85	**25.46**
house256	disk	30.75	29.50	**32.02**	31.88
	motion	29.78	27.28	30.87	**31.03**
	gaussian	30.72	30.54	31.19	**31.52**
	box	29.48	28.66	30.34	**30.79**
fingerprint512	disk	26.87	24.66	27.45	**27.53**
	motion	23.82	22.16	24.91	**25.46**
	gaussian	27.67	27.21	28.08	**28.19**
	box	22.85	22.69	24.02	**24.28**
Barbara512	disk	24.28	24.30	**25.28**	24.72
	motion	24.10	23.73	**25.01**	24.39
	gaussian	24.27	24.15	**24.43**	24.39
	box	23.69	23.54	**24.01**	23.91
Lena512	disk	31.13	28.95	31.72	**31.82**
	motion	29.77	27.45	30.30	**30.42**
	gaussian	31.53	30.63	32.15	**32.17**
	box	29.17	28.18	29.35	**29.75**

TABLE 4.2

Comparison of the PSNR values (dB) of the results from the four algorithms, with respect to the noise level $\sigma = 5$.

with only small modifications. In the end of the experimental section, we demonstrated some examples of applying Algorithm 2 on image de-noising and image in-painting. For image de-noising, the matrix A in the model (3.9) becomes the identical matrix and for image in-painting, the matrix A in the model (3.9) becomes a diagonal matrix with diagonal element being 1 if the corresponding pixel is known or 0 otherwise. See Figure 4.5 for the visual illustration of the result de-noised by the model (2.5) using 3-level liner spline wavelet frame and the one using the non-local wavelet frame (3.8). See Figure 4.6 and Figure 4.7 for the comparisons of the in-painted results by the linear spline wavelet approach and the non-local wavelet frame approach. It is seen that the non-local wavelet tight frame (3.8) performed better than the linear spline framelet on the tested images.

4.2. Summary. The performance of a regularization-based image restoration method largely depends on not only the accuracy but also the strength of the assump-

tions used for regularizing the true image. In recent years, the wavelet tight frame based regularization plays an active role in the newest development of powerful image restoration methods, which seek the solution that minimizes the ℓ_1 norm of the associated wavelet tight frame coefficients. The wavelet tight frame approach assumes that the interest image is likely to have sparse approximation in the wavelet tight frame domain, which essentially exploits the sparse nature of local image intensity variations. However, in existing wavelet tight frame systems, there is no measurement on the self-similarity relationship of image structure over the whole image domain, one often seen phenomena in natural images of complex textures. By exploiting such non-local self-similarities, the patch-based methods like BM3D or the non-local mean methods demonstrated the promising performance in various image restoration tasks.

Motivated by the idea behind these non-local approaches, we developed in this paper a scheme of constructing non-local wavelet frame and tight frame that are adaptive to the input image. The constructed adaptive non-local wavelet frame is composed of two types of wavelet frame systems: one local version and one nonlocal version of some existing wavelet frame system. The proposed wavelet frame system not only measures the local variations on image intensity, but also the global similarities of image structures over the whole image. As such, the ℓ_1 norm based regularization under the proposed non-local wavelet frame can simultaneously exploits these two priors: the local sparsity prior of local image intensity variations and the global self-recursive prior of image structures. Compared to the existing wavelet tight frame based approaches, our approach has better performance owing to the usage of an additional powerful prior. Compared to the existing non-local approaches, our approach has a variational formulation applicable to general image restoration problems and performs consistently over a wide range of images including those lacks the self-similar image structures. The experiments on image de-convolution also showed the advantages of our approaches over some related local and non-local approaches.

REFERENCES

[1] I. Daubechies. *Ten lectures on wavelets.* CBMS-NSF Lecture Notes, SIAM, 1 edition, 1992.

[2] Stéphane Mallat. *A wavelet tour of signal processing.* Academic Press Inc., San Diego, CA, third edition, 2009.

[3] A. Ron and Z. Shen. Affine system in $L_2(R^d)$: the analysis of the analysis operator. *J. of Func. Anal.*, 148, 1997.

[4] I. Daubechies, B. Han, A. Ron, and Z. Shen. Framelets: MRA-based constructions of wavelet frames. *Appl. Comput. Harmon. Anal.*, 14:1–46, 2003.

[5] Z. Shen. Wavelet frames and image restorations. *Proceedings of the International Congress of Mathematicians, Hyderabad, India*, 2010.

[6] D. Donoho. De-noising by soft thresholding. *IEEE Trans. Inf. Theory*, 41(3):613–627, 1995.

[7] E. Candes and D. L. Donoho. New tight frames of curvelets and optimal representations of objects with piecewise-C^2 singularities. *Comm. Pure Appl. Math*, 57:219–266, 2002.

[8] J. Starck, E. Candes, and D. Donoho. The curvelet transform for image denoisi. *IEEE Trans. Image Proc.*, 11(6):670–684, 2002.

[9] J. Cai, H. Ji, C. Liu, and Z. Shen. High-quality curvelet-based motion deblurring using an image pair. In *IEEE CVPR*, 2009.

[10] S. Mallat and E. Lepennec. Sparse geometric image representation with bandelets. *IEEE Transactions on Image Processing*, 14:423–438, 2005.

[11] E. Pennec and S. Mallat. Bandlet image approximation and compression. *SIAM Multiscale Model. Simul.*, 4(3):992–1039, 2005.

[12] J.-F. Cai, R. Chan, and Z. Shen. A framelet-based image inpainting algorithm. *Appl. Comput. Harmon. Anal.*, 24:131–149, 2008.

[13] J. Cai, H. Ji, C. Liu, and Z. Shen. Framelet based blind image deblurring from a single image. *IEEE Trans. Image Proc.*, 21(2):562–572, 2012.

[14] B. Dong, H. Ji, J. Li, and Z. Shen. Wavelet frame based blind image inpainting. *Appl. Comput. Harmon. Anal.*, 32(2):268–279, 2012.
[15] L. Rudin, S. Osher, and E. Fatemi. Nonllienar total variation based noise removal algorithms. *Phys. D.*, 60:259–268, 1992.
[16] J. Cai, B. Dong, Z. Shen, and S. Osher. Image restoration: total variation; wavelet frames; and beyond. *Journal of the American Mathematical Society*, 25(4):1033–1089, 2012.
[17] M. Elad and M. Ahron. Image denoising via sparse and redundant representations over learned distionaries. *IEEE Trans. on Image Processing*, 54(12):3736–3745, 2006.
[18] J. Cai, S Huang, Z. Shen, and G. Ye. Data-driven tight frame construction and image denoising. Technical report, UCLA-CAM report 12-40, 2012.
[19] A. Buades, B. Coll, and J.M. Morel. A non-local algorithm for image denoising. In *CVPR*, pages 60–65, 2005.
[20] G. Gilboa and S. Osher. Nonlocal operators with applications to image processing. *SIAM Multiscale Model. Simul.*, 7(3):1005–1028, 2008.
[21] G. Peyre, S. Bougleux, and L. Cohen. Non-local regularization of inverse problems. In *ECCV*, 2008.
[22] Y. Lou, X. Zhang, S. Osher, and A. Bertozzi. Image recovery via nonlocal operators. *Journal of Scientific Computing*, 42(2):185–197, 2010.
[23] X. Zhang, M. Burger, X. Bresson, and S. Osher. Bregmanized nonlocal regularization for deconvolution and sparse reconstruction. *SIAM*, 3(3):253–276, 2010.
[24] K. Dabov, A. Foi, V. Katkovnik, and K. Egiazarian. Image denoising by sparse 3-d transform-domain collaborative filtering. *Image Processing, IEEE Transactions on*, 16(8):2080–2095, 2007.
[25] K. Dabov, A. Foi, K. Katkovnik, and K. E. Image restoration by sparse 3d transform-domain collaborative filtering. *SPIE Electronic Imaging*, 6812, 2008.
[26] A. Danielyan, V. Katkovnik, and K. Egiazarian. Bm3d frames and variational image deblurring. *IEEE Trans. Image Proc.*, 21(4):1715–1728, 2012.
[27] J. Mairal, F. Bach, J. Ponce, G. Sapiro, and A. Zisserman. Non-local sparse models for image restoration. In *ICCV*, 2011.
[28] T. Goldstein and S. Osher. The split bregman method for l1-regularized problems. *SIAM J. Img. Sci.*, 2(2):323–343, 2009.
[29] J.F. Cai, S. Osher, and Z. Shen. Split bregman methods and frame based image restoration. *SIAM Multiscale Model. Simul.*, 8(2):337–369, 2009.
[30] B. Dong and Z. Shen. MRA based wavelet frames and applications. *IAS Lecture Notes Series, Summer Program on "The Mathematics of Image Processing", Park City Mathematics Institute*, 2010.
[31] A. Chai and Z. Shen. Deconvolution: A wavelet frame approach. *Numer. Math.*, 106:529–587, 2007.
[32] J.-F. Cai, H. Ji, C. Liu, and Z. Shen. Blind motion deblurring from a single image using sparse approximation. In *CVPR*, 2009.
[33] M. Elad, P. Milanfar, and R. Rubinstein. Analysis versus synthesis in signal priors. *Inverse Problems*, 23(3):947–968, 2007.
[34] D. Donoho and I. Johnstone. Adapting to unknown smoothness via wavelet shrinkage. *J. Amer. Statist. Assoc.*, 90:1200–1224, 1995.

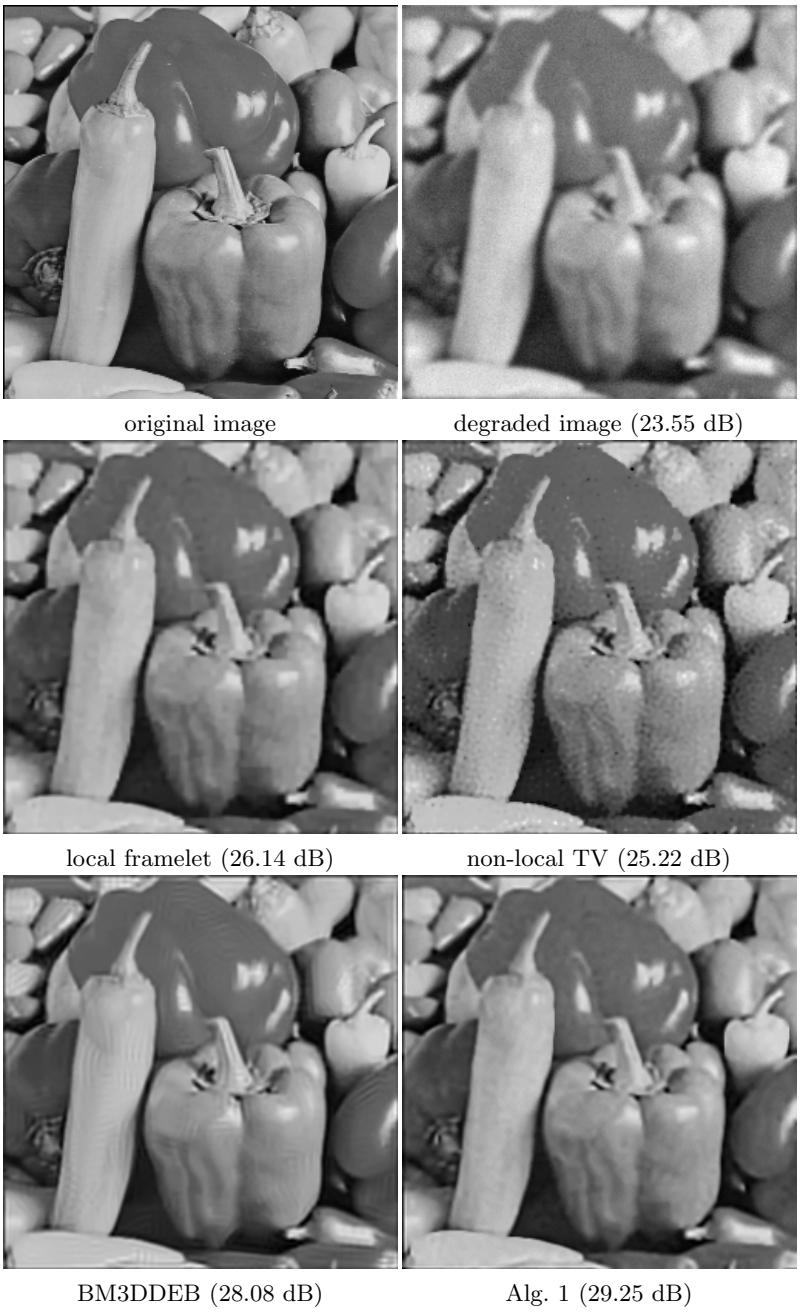

FIG. 4.2. *Visual comparison of de-blurred results for the image "peppers256". The true image is degraded by the* 25×25 *Gaussian kernel with standard deviation* 1.6 *and the Gaussian noise with standard deviation* $\sigma = 5$.

original image

degraded image (20.57 dB)

local framelet (25.43 dB)

non-local TV (25.43 dB)

BM3DDEB (26.50 dB)

Alg. 1 (26.82 dB)

FIG. 4.3. *Visual comparison of de-blurred results for the image "cameraman256". The true image is degraded by the 9×9 box kernel and the Gaussian noise with standard deviation* $\sigma = 5$.

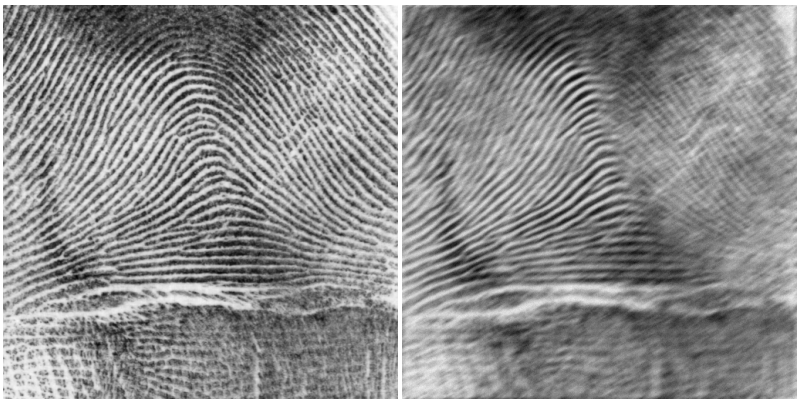

original image

degraded image (18.02 dB)

local framelet (26.87 dB)

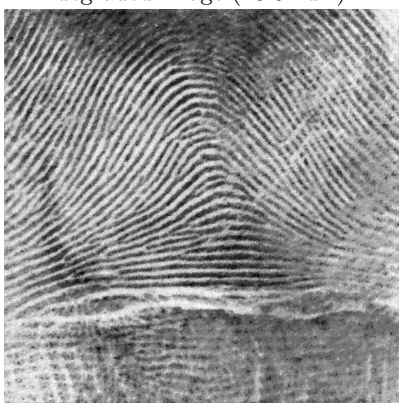

non-local TV (24.66 dB)

BM3DDEB (24.66 dB)

Alg. 1 (27.53 dB)

FIG. 4.4. *Visual comparison of de-blurred results for the image "fingerprint512". The true image is degraded by the* 9×15 *motion kernel and the Gaussian noise with standard deviation* $\sigma = 5$.

noisy image (22.10 dB) linear spline framelet (30.78 dB) Alg. 2 (32.21 dB)

FIG. 4.5. *Visual comparison of de-noised results for the image "Lena512". The true image is degraded by Gaussian noise with standard deviation* 20.

damaged image linear spline framelet (28.64 dB) Alg. 2 (30.02 dB)

FIG. 4.6. *Visual comparison of in-painted results for the image "boat256". The forty percents of image pixels of the true image are randomly missing.*

damaged image linear spline framelet (34.38 dB) Alg. 2 (35.21 dB)

FIG. 4.7. *Visual comparison of in-painted results for the image "Lena512". Some image pixels of the true image are completed damaged by the scratches and texts.*